

## **Calculation method for the in-plane carrying capacity of low-rise reinforced concrete walls used in nuclear safety structures**

**\*Xin-Bo Li<sup>1)</sup>, Shu-Heng Guo<sup>2)</sup>, Xing-Yi Wu<sup>3)</sup>, and Jin-Xin Gong<sup>4)</sup>**

*1), 2), 3), 4) State Key Laboratory of Coastal and Offshore Engineering, Dalian University of Technology, Dalian 116024, China*

*4) [jinxingong@163.com](mailto:jinxingong@163.com)*

### **ABSTRACT**

This paper investigates the calculation method for the lateral carrying capacity of the low-rise reinforced concrete wall used in nuclear safety-related structures. First, a composite mechanical model that considers a diagonal shear surface inside the wall and a friction surface at the bottom of the wall is established based on the failure mode of low-rise reinforced concrete wall specimens in tests. Then, a calculation equation for lateral carrying capacity is derived from the proposed model with the application of the plastic limit theory. Based on test results, the proposed equation is simplified and calibrated, yielding a simplified design equation of the lateral carrying capacity for the low-rise reinforced concrete wall. The comparison between calculated and experimental results indicates that the calculation results obtained by the proposed method show good agreement with the test results, and the computational accuracy is better than that of the method suggested in the codes ACI 349 and RCC-CW 2015.

### **1. INTRODUCTION**

Nuclear safety-related concrete structures are support and shielding structures in nuclear power plants with the primary function of protecting nuclear safety-grade systems and components. Under seismic loading, the nuclear safety-related structure is subjected to a lateral force in line with the seismic direction, i.e., in-plane shear. Although both the reinforced concrete shear walls used in ordinary housing construction and the nuclear safety-related structure are subjected to in-plane lateral shear forces, their force patterns and mechanisms are significantly different. The shear walls of ordinary housing construction are only used in high-rise buildings and are mainly subjected to in-plane

---

<sup>1)</sup> Graduate Student

<sup>2)</sup> Graduate Student

<sup>3)</sup> Graduate Student

<sup>4)</sup> Professor

bending under seismic action, while the nuclear safety-related structure in nuclear power plants are low-rise walls and are mainly subjected to in-plane shear under seismic action. Therefore, the calculation method for the lateral carrying capacity of the low-rise reinforced concrete wall in nuclear power plants is different from that of the reinforced concrete shear walls in ordinary housing construction.

In the past decades, extensive experimental studies have been conducted on low-rise reinforced concrete walls (Lefas and Kotsovos, 1990, Gulec et al., 2008, Ji et al., 2018, Baek et al., 2020, Nie et al., 2020), and calculation methods for the in-plane lateral carrying capacity have been proposed. Hus et al. (1985) calculated the lateral carrying capacity of low-rise reinforced concrete walls based on the softened truss model. Kassem et al. (2015) and Hwang et al. (2002) discussed the calculation method for the lateral carrying capacity of low-rise reinforced concrete walls using the strut-and-tie model. Gulec et al. (2011) established an empirical equation for calculating the lateral carrying capacity of low-rise reinforced concrete walls based on a large amount of experimental data, which was adopted by design standards such as ASCE/SEI 43-05 (ASCE/SEI 43-05, 2005), RCC-CW 2015 (RCC-CW, 2015), and NB/T 20488-2018 (NB/T 20488-2018, 2018). In addition, the design codes ACI 349-13 (ACI 349-13, 2013) and ASCE/SEI 43-19 adopt the regulations and equations in ACI 318-08 (ACI 318-08, 2018) to calculate the in-plane shear carrying capacity of reinforced concrete walls.

The calculation equation for the lateral carrying capacity of low-rise reinforced concrete walls proposed by Gulec et al. (2011) is purely empirical, and the reinforcement ratio in both directions is determined according to the height-to-width ratio of the wall. The equations used in codes ACI 349 and ASCE/SEI 43-19 are based on those in the building design code, and the effect of vertical reinforcement in the equations is ignored. For the shear walls used in ordinary housing construction, the amount of vertical reinforcement is determined by the bending moment generated by the lateral loading. If the wall is configured with sufficient vertical reinforcement, the vertical reinforcement will not yield when shear failure occurs. However, for low-rise reinforced concrete walls used in nuclear safety-related structures, the calculation of the bending capacity is usually not performed in the design. If the lateral force is large, a significant bending moment will also be generated in the wall, causing a considerable amount of vertical reinforcement to yield. Gong et al. (2022) used the finite element analysis method based on a modified compression field theory to analyze 107 low-rise reinforced concrete walls with height-to-width ratios ranging from 0.25 to 2.0, and the results showed that 80 specimens did not yield in the horizontal direction but yielded in the vertical direction, 20 specimens yielded in both the horizontal and vertical directions, and 7 specimens were not configured with vertical reinforcement or the vertical reinforcement did not yield. Although the test specimens are not fully representative of the low-rise reinforced concrete wall in the actual project, they also illustrate to some extent that the vertical reinforcement in low-rise reinforced concrete walls may also yield under in-plane lateral loading. Therefore, it is not reasonable to consider only the yielding of the reinforcement in the horizontal direction in the design equations. In this work, a mechanical model for the in-plane carrying capacity of the low-rise reinforced concrete wall is established. Combining the plastic limit theory and experimental results, a calculation equation for the lateral carrying capacity of the low-rise reinforced concrete wall is presented.

## 2. Mechanical model and basic equation

### 2.1 Plastic limit theory

The plastic limit theory is a common method for the ultimate load capacity analysis of reinforced concrete structures or members, such as the plastic limit analysis of reinforced concrete slabs. In the plastic limit theory, the constitutive relationship of the material takes the form of rigid-perfect plastic, as shown in Fig. 1. This theory assumes that the material of the structure at the limit state is either in a rigid state (no elastic deformation) or in a completely plastic flow state (deformation is entirely plastic). In fact, neither steel nor concrete is an ideal rigid-perfect plastic material. However, reinforced concrete structures or members undergo a very short elastic phase when they reach their ultimate state, and most of the deformation is in the plastic phase. Therefore, it is feasible to approximate that reinforcement and concrete are rigid-plastic materials. Under this assumption, the structure goes directly from the rigid state to the fully plastic flow state, and the stresses of the material remain constant during the plastic phase. In this way, the analysis of the load-carrying capacity of the reinforced concrete structure or member can be completed in one step, omitting the analysis of the elastic phase and the consideration of the stress changes of the reinforcement and concrete in the elasto-plastic phase. Therefore, the analysis process can be greatly simplified.

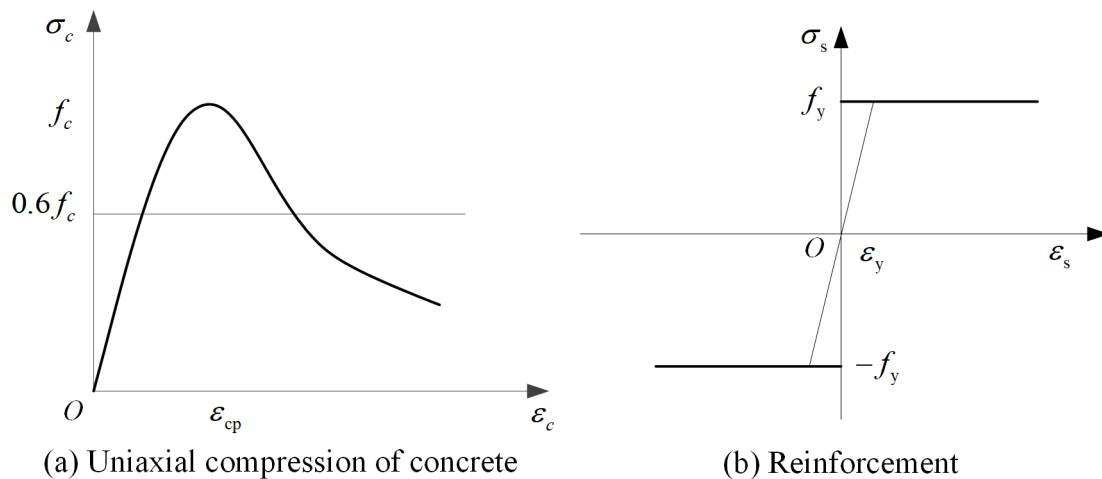


Fig. 1 Rigid-perfect plastic constitutive relationship of concrete and reinforcement

### 2.2 Mechanical model of the low-rise reinforced concrete wall

The low-rise reinforced concrete wall will be subjected to both bending moments and shear forces under lateral loading. Fig. 2(a) shows the shear failure model of the wall based on the test results (Gong et al., 2022). In the Fig. 2(a), AB is a main shear crack with a downward projection length of  $h/k$  ( $k = \tan \theta$ , and  $\theta$  is the angle of the diagonal crack with the x-axis). BC is a shear friction crack along the wall and base with a length of  $l - h/k$ . Fig. 2(b) shows the stress state of the concrete and reinforcement in both directions in a small element on the diagonal crack AB, and Fig. 2(c) displays the stress state of the concrete on the shear friction surface.

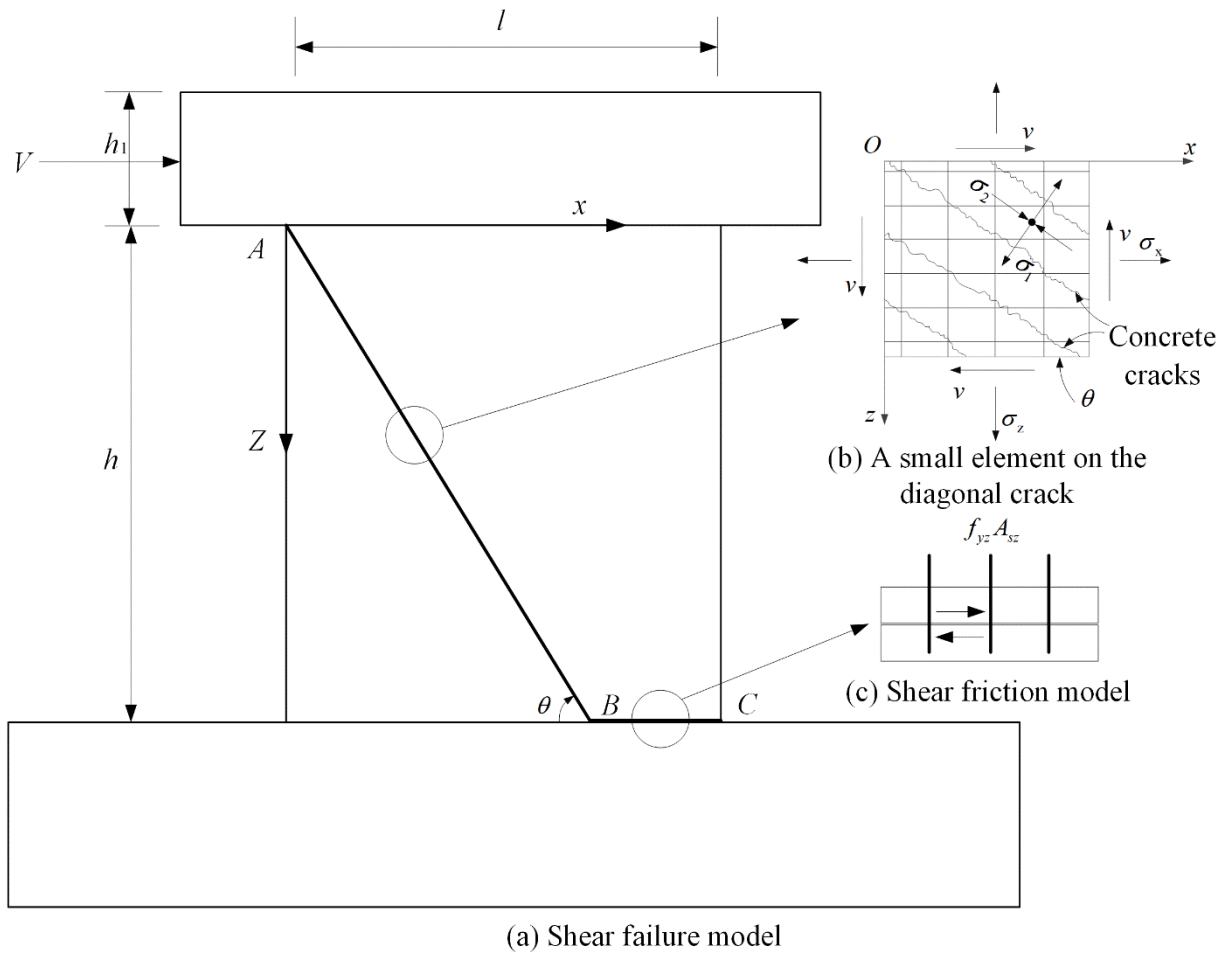


Fig. 2 Failure mode of low-rise reinforced concrete walls under lateral loading

### 2.3 Shear force on the diagonal shear surface

As shown in Fig. 2, when considering the carrying capacity of a low-rise reinforced concrete wall according to the shear failure mode, the carrying capacity consists of two parts, including the shear force carried by the truss composed of reinforcement and concrete at the diagonal crack AB and the shear force carried by the shear friction at the crack BC. For the reinforced concrete element on the diagonal crack AB (shown in Fig. 2b), our previous work has proposed the calculation equation of the shear stress that the element can withstand by plastic limit analysis (Gong et al., 2018):

$$v(\theta) = \frac{c \cos \varphi}{\sin(2\theta)} + (\rho_x f_{yx} - \sigma_x) \frac{\sin \varphi - \cos(2\theta)}{2 \sin(2\theta)} + [\rho_z f_{yz} - \sigma_z(x)] \frac{\sin \varphi + \cos(2\theta)}{2 \sin(2\theta)} \quad (1)$$

where  $\rho_x$  and  $f_{yx}$  are the reinforcement ratio and yield strength of the reinforcement in the x-direction (horizontal direction), respectively;  $\rho_z$  and  $f_{yz}$  are the reinforcement ratio and yield strength of the reinforcement in the z-direction (vertical direction);  $\sigma_x$  and

$\sigma_z(x)$  are the stresses in the x and z directions, respectively;  $c$  and  $\varphi$  are the cohesion and the angle of internal friction of the concrete in the Mohr-Coulomb criterion, which have the following relationships with the equivalent tensile strength  $f'_t$  and equivalent compressive strength  $f'_c$  of the concrete:

$$c = \frac{f'_c(1 - \sin \varphi)}{2 \cos \varphi} = \frac{1}{2} \sqrt{f'_c f'_t} \quad (2)$$

$$\sin \varphi = \frac{f'_c - f'_t}{f'_c + f'_t} \quad (3)$$

Compared to the compressive strength of the concrete, the tensile strength of the concrete is very low, so  $f'_t = 0$ . According to Eqs. (2) and (3),  $c = 0$ ,  $\sin \varphi = 1$ , and the following equation can be obtained:

$$\frac{1 - \cos(2\theta)}{2 \sin(2\theta)} = \frac{\sin^2 \theta + \cos^2 \theta - \cos^2 \theta + \sin^2 \theta}{4 \sin \theta \cos \theta} = \frac{2 \sin^2 \theta}{4 \sin \theta \cos \theta} = \frac{1}{2} \tan \theta = \frac{1}{2} k \quad (4a)$$

$$\frac{1 + \cos(2\theta)}{2 \sin(2\theta)} = \frac{\sin^2 \theta + \cos^2 \theta + \cos^2 \theta - \sin^2 \theta}{4 \sin \theta \cos \theta} = \frac{2 \cos^2 \theta}{4 \sin \theta \cos \theta} = \frac{1}{2} \cot \theta = \frac{1}{2k} \quad (4b)$$

Therefore, Eq. (1) can be expressed as:

$$v_1(x) = \frac{1}{2} k (\rho_x f_{yx} - \sigma_x) f_{yx} + \frac{1}{2k} [\rho_z f_{yz} - \sigma_z(x)] \quad (5)$$

Under the assumption of rigid-perfect plastic, it is assumed that the stress distribution in the z-direction of the wall can be expressed as the following form (as shown in Fig. 3):

$$\sigma_z(x) = q_1 + \frac{x}{l} (q_2 - q_1) \quad (6)$$

where  $q_1 = -\frac{N}{A_c} + \frac{hV_c}{2W}$ ;  $q_2 = -\frac{N}{A_c} - \frac{hV_c}{2W}$ ;  $W = bl^2/6$ ;  $h$ ,  $l$ , and  $b$  represent the height, width and thickness of the wall, respectively;  $A_c$  is the area of the horizontal section of the wall;  $N$  is the vertical load acting on the wall;  $V_c$  is the lateral force on the wall.

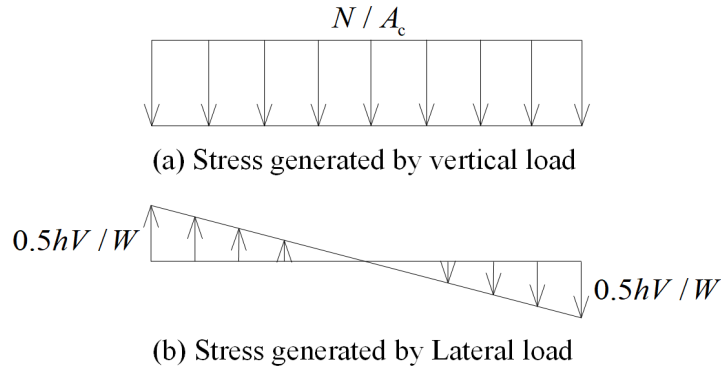


Fig. 3 Stress in the vertical direction (z-direction) of the wall

It should be noted that the vertical stress of the wall shown in Fig. 3 does not exactly match the actual situation. Theoretically, the distribution of vertical stress in the wall needs to be calculated based on the distribution of vertical strain along the horizontal direction and the stress-strain relationship of the concrete. However, for the low-rise reinforced concrete wall, the strain distribution in the cross-section no longer conforms to the plane cross-section assumption, and the strain distribution in the cross-section of the wall is unknown. Therefore, it is difficult to obtain an accurate distribution of the vertical stresses in the wall. Although the calculation equation for the lateral carrying capacity of the wall obtained from Eq. (6) is approximate, it has a simple form and is also convenient for application. What's more, the computational accuracy of the equation can be guaranteed after using the experimental data for modification.

The external lateral stress of the wall is  $\sigma_x = 0$ . According to Eq. (4), the shear force carried by the diagonal shear surface AB is as follows:

$$V_{AB} = \int_0^{h/k} v_1(x) dx = b \int_0^{h/k} \left\{ \frac{1}{2} k (\rho_x f_{yx} - \sigma_x) + \frac{1}{2k} [\rho_z f_{yz} - \sigma_z(x)] \right\} dx \quad (7)$$

Substituting Eq. (5) into Eq. (7) and integrating it yields Eq. (8) as follows:

$$V_{AB} = \frac{b}{2} \left[ \frac{3h^3 V_c}{l^3 b k^3} + \rho_x f_{yx} h - \sigma_x h + \frac{h}{k^2} \left( \rho_z f_{yz} + \frac{N}{A_c} - 3 \frac{h V_c}{b l^2} \right) \right] \quad (8)$$

#### 2.4 Shear force on the shear friction surface

For the shear friction surface shown in Fig. 2(c), the shear capacity under vertical compressive stress is provided by the internal cohesion and the friction force of the concrete, as well as the dowel stress of the reinforcement perpendicular to the shear surface. Referring to the Eurocode (EN 1992-1-1:2004), the shear stress of concrete and reinforcement on the shear friction surface can be calculated by the following equation:

$$v_2 = c_1 f_{ct} + \mu \sigma_n + \rho f_y (\mu \sin \alpha + \cos \alpha) \leq 0.5 v f_c \quad (9a)$$

where  $c_1$  is the calculation parameter;  $f_{ct}$  is the tensile strength of the concrete;  $f_c$  is the compressive strength of the concrete;  $f_y$  is the yield strength of the reinforcement that intersects with the shear friction surface;  $\sigma_n$  is the minimum normal stress across the shear friction surface ( $\sigma_n < 0.6 f_c$ , and with the compression as positive and the tension as negative), and  $c f_{ct} = 0$  when  $\sigma_n$  is a tensile stress;  $A_s$  is the area of the reinforcement that crosses the shear friction surface;  $\alpha$  is the area of the reinforcement that intersects the shear friction surface, and  $45^\circ \leq \alpha \leq 90^\circ$ ;  $v$  is the effective coefficient;  $\mu$  is the coefficient related to the roughness of the shear friction surface.

In this study,  $\alpha = 90^\circ$ ,  $f_{ct} = f_t$ ,  $f_y = f_{yz}$ , and  $\rho = \rho_z$ . Meanwhile, considering that  $\sigma_n$  is positive when under compression, i.e.,  $\sigma_n = -\sigma_z(x)$ , so Eq. (9) can be rewritten as:

$$v_2(x) = c_1 f_t + \mu [-\sigma_z(x) + \rho_z f_{yz}] \quad (9b)$$

Therefore, the shear force carried by the shear friction surface BC can be calculated as follows:

$$\begin{aligned} V_{BC} &= \int_{h/k}^l v_2(x) dx = \int_{h/k}^l \{c_1 f_t + \mu [-\sigma_z(x) + \rho_z f_{yz}]\} dx \\ &= 3 \frac{\mu h^2 V_c}{kl^2} \left(1 - \frac{h}{kl}\right) + b \left(c_1 f_t + \mu \rho_z f_{yz} + \mu \frac{N}{A_c}\right) \left(l - \frac{h}{k}\right) \end{aligned} \quad (10)$$

### 2.5 Total lateral force of the wall

The total lateral force that the wall can withstand is  $V_c = V_{AB} + V_{BC}$ . Substituting Eqs. (8) and (10) yields:

$$V_c = \frac{bh}{2k^2} \left[ \rho_z f_{yz} + \frac{N}{A_c} + (\rho_x f_{yx} - \sigma_x) k^2 \right] + b \left( l - \frac{h}{k} \right) \left( c_1 f_t + \mu \frac{N}{A_c} + \rho_z f_{yz} \mu \right) \quad (11)$$

$$\frac{3(2k\mu - 1) \left( \frac{h}{l} \right)^2 \left( \frac{h}{l} - k \right) + 1}{2k^3}$$

Eq. (11) is the upper limit solution obtained according to the plastic limit theory, and the minimum value of this equation is the solution closest to the theoretical solution. Taking a set of parameters from the Eurocode, i.e.,  $c_1 = 0.25$  and  $\mu = 0.5$ , Eq. (11) can be expressed as:

$$\frac{V_c}{bh_2\rho_z f_{yz}} = \frac{\frac{1}{2k^2} \left( 1 + \frac{N}{A_c \rho_z f_{yz}} + \frac{\rho_x f_{yx} - \sigma_x}{\rho_z f_{yz}} k^2 \right)}{\frac{3}{2k^3} \left( \frac{h}{l} \right)^2 \left( \frac{h}{l} - k \right) (k-1) + 1} + \frac{\left( \frac{l}{h} - \frac{1}{k} \right) \left( 0.25 \frac{f_t}{\rho_z f_{yz}} + 0.5 \frac{N}{A_c \rho_z f_{yz}} + 0.5 \right)}{\frac{3}{2k^3} \left( \frac{h}{l} \right)^2 \left( \frac{h}{l} - k \right) (k-1) + 1} \quad (12)$$

Taking values in the range of variables that are commonly used in engineering,  $\frac{N}{A_c \rho_z f_{yz}} = -0.3 \sim 0.5$ ,  $\frac{\rho_x f_{yx}}{\rho_z f_{yz}} = 0.5 \sim 2.0$ ,  $\frac{h}{l} = 0.3 \sim 1.0$ , and  $\frac{f_t}{\rho_z f_{yz}} = 0.3$ . Then the one-dimensional search method is used to find the  $k$  that makes Eq. (12) have the minimum value. The results show that within the range of values of the above variables, the  $k$  that minimizes Eq. (12) is in the range of 1.35 to 1.76.

Obviously, it is very inconvenient to obtain the in-plane lateral carrying capacity of low-rise reinforced concrete walls by finding the minimum value of Eq. (12) in engineering design, so it needs to be simplified.

### 3 Simplification and calibration of the equation

#### 3.1 Simplification for the denominator term of the equation

The denominator term of Eq. (12) can be expressed as:

$$K = \frac{3}{2k^3} \left( \frac{h}{l} \right)^2 \left( \frac{h}{l} - k \right) (k-1) + 1 \quad (13)$$

For the low-rise reinforced concrete wall studied in this paper, the values of height-to-width ratio  $h/l$  range from 0.25 to 2.0. Fig. 4 exhibits the variation of  $K$  when  $k$  is varied in the range of  $h/l \sim 2.0$ . As can be seen from Fig. 4, the variation of  $K$  is small in the range of  $h/l \sim 2.0$ . Therefore, it can be approximated that  $K$  does not change with  $k$ . Thus, Eq. (13) can be simplified to a function independent of  $k$ , which has the following form:

$$K = x \left( \frac{h}{l} \right)^2 + 1 \quad (14)$$

where  $x$  is the coefficient that needs to be determined from the experimental data.



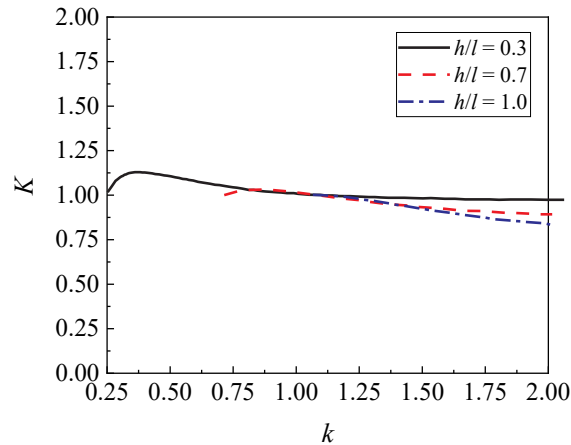


Fig. 4 Variation of  $K$  with  $k$

### 3.2 Simplification for the numerator term of the equation

Since it is approximated that the denominator term in Eq. (12) does not change with  $k$  in the range of variables commonly used in engineering, finding the  $k$  that minimizes the numerator term of Eq. (12) can make Eq. (12) obtain the minimum  $k$ . Taking the derivative of the numerator term of Eq. (12) and making the result equal to 0, the following equation can be obtained:

$$k = \frac{\rho_z f_{yz} + \frac{N}{A_c}}{0.25 f_t + 0.5 \frac{N}{A_c} + 0.5 \rho_z f_{yz}} \quad (15)$$

Substituting Eq. (15) into the numerator term of Eq. (12) and simplifying it yields the following equation:

$$V_{cn} = 0.5b \left[ h(\rho_x f_{yx} - \sigma_x) + (l - 0.25h) \left( 0.5 f_t + \frac{N}{A_c} + \rho_z f_{yz} \right) \right] - \frac{bh}{2} \left[ \frac{0.0625 f_t^2}{\rho_z f_{yz} + \frac{N}{A_c}} + 0.125 f_t \right] \quad (16)$$

The last term in Eq. (16) is very small and can be ignored. Therefore, the calculation equation for the lateral carrying capacity of the low-rise reinforced concrete wall can be simplified as follows:

$$V_c = \frac{V_{cn}}{K} = \frac{0.5bh \left[ \rho_x f_{yx} - \sigma_x + \left( \frac{l}{h} - 0.25 \right) \left( 0.5f_t + \frac{N}{A_c} + \rho_z f_{yz} \right) \right]}{x \left( \frac{h}{l} \right)^2 + 1} \quad (17)$$

### 3.3 Determination of parameters in the simplified equation

According to the collected test results of 107 reinforced concrete walls with height-to-width ratios ranging from 0.25 to 2.0 (Gong et al., 2022), the parameter  $x$  in Eq. (17) is determined, and  $x = 0.5$ . Therefore, the calculation equation for the lateral carrying capacity of the low-rise reinforced concrete wall under vertical compression can be expressed as:

$$V_c = \frac{0.5bh \left[ \rho_x f_{yx} - \sigma_x + \left( \frac{l}{h} - 0.25 \right) \left( 0.5f_t + \frac{N}{A_c} + \rho_z f_{yz} \right) \right]}{0.5 \left( \frac{h}{l} \right)^2 + 1} \quad (18)$$

## 4 Verification of the calculation equation

### 4.1 Calculation of the lateral carrying capacity of the low-rise wall under vertical compression

According to Eq. (18) in this paper and the relevant equations in the codes ACI 349-13 and RCC-CW 2015, the lateral carrying capacity of 107 low-rise reinforced concrete walls is calculated under vertical compression, respectively. Table 1 shows the comparison of the calculated results with the experimental results. Fig. 5 shows the distribution of the ratio of the calculated results of the lateral carrying capacity to the test results. It can be seen from Table 1 and Fig. 5 that the lateral carrying capacity calculated by the proposed equation is closest to the mean value of the lateral carrying capacity obtained from the test, and the coefficient of variation (COV) is the smallest. In addition, the ratio of the lateral carrying capacity calculated by the proposed equation to the test results shows the smallest fluctuation with respect to the horizontal line of 1.0.

Table 1 Comparison of calculated and experimental results for the low-rise wall under compressive and lateral loading.

Ratio	Mean	Median	Standard deviation	COV	Minimum	Maximum
$V_{paper}/V_{exp}$	0.996	1.029	0.203	0.204	0.566	1.468
$V_{ACI}/V_{exp}$	1.077	1.048	0.367	0.341	0.459	2.124
$V_{RCC}/V_{exp}$	1.529	1.600	0.382	0.250	0.597	2.360

Note:  $V_{paper}$  represents the result calculated by the proposed equation;  $V_{exp}$  represents the experimental results;  $V_{ACI}$  and  $V_{RCC}$  represent the result calculated by the equations in the codes ACI 349-13 and RCC-CW 2015, respectively.

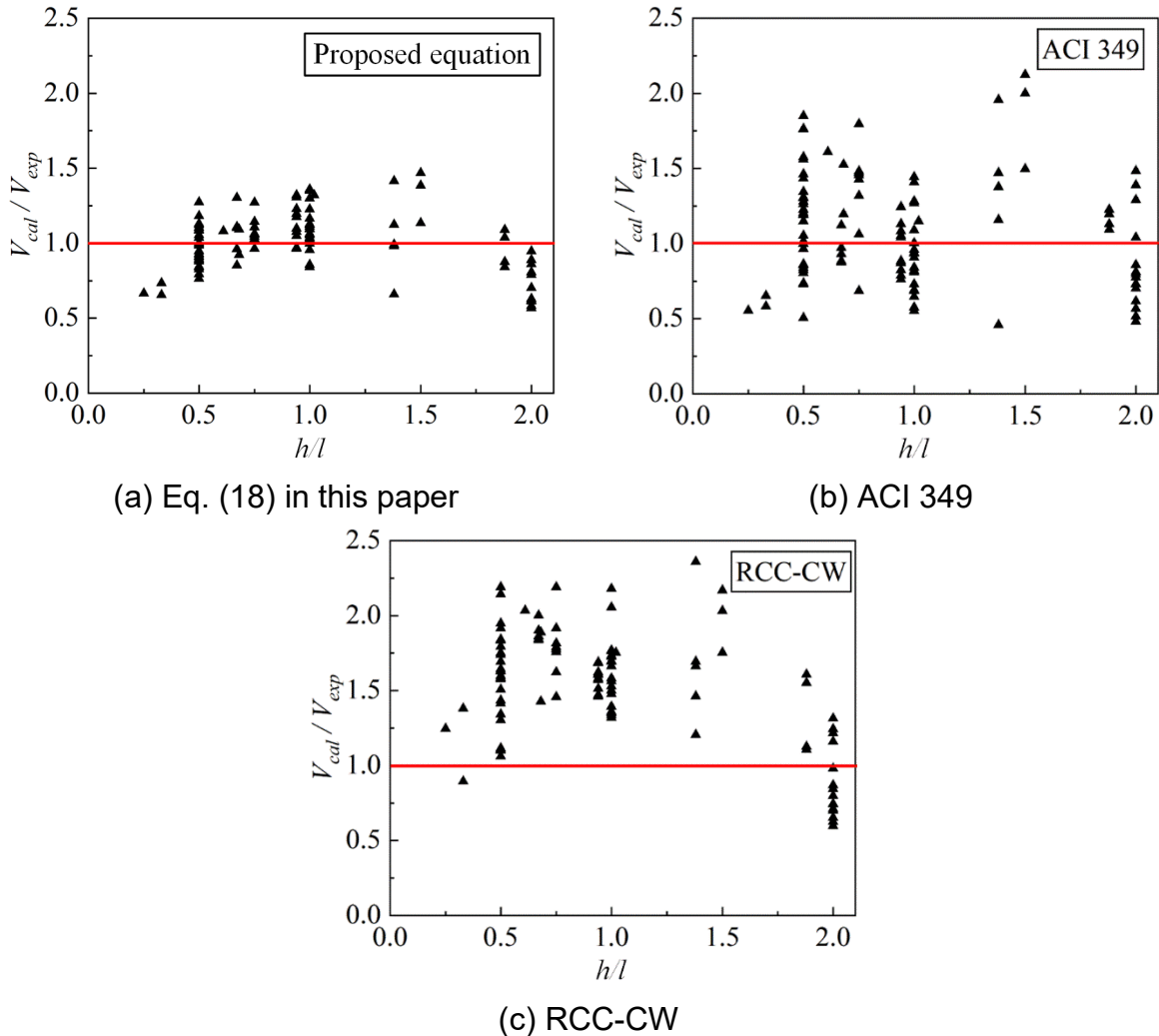


Fig. 5 Distribution of the ratio of calculated results to experimental results for the wall under vertical compression.

#### 4.2 Calculation of the lateral carrying capacity of walls under vertical tension

The nuclear safety-related concrete structure in nuclear power plants may be subjected to both lateral and upward seismic loads, in which case the lateral carrying capacity of the wall under vertical tension needs to be calculated. The experimental results of 25 low-rise reinforced concrete walls with a height-to-width ratio ranging from 0.9 to 1.3 under vertical tension and lateral forces are collected from the relevant literature (Gong et al., 2022). Similarly, the lateral carrying capacity of the wall under such load conditions is calculated with Eq. (18). It should be noted that since the wall is subjected to vertical tension,  $N$  is negative in the calculation. As can be seen from

Table 2 and Fig. 6, the calculation results obtained by using the proposed equation for the lateral carrying capacity of the low-rise reinforced concrete wall under vertical tension are closest to the experimental results.

Table 2 Comparison of calculated and experimental results for the wall under tensile and lateral loading.

Ratio	Mean	Median	Standard deviation	COV	Minimum	Maximum
$V_{paper}/V_{exp}$	0.943	0.911	0.194	0.206	0.681	1.483
$V_{ACI}/V_{exp}$	0.750	0.695	0.344	0.459	0.307	1.614
$V_{RCC}/V_{exp}$	1.777	1.572	0.717	0.404	0.958	4.065

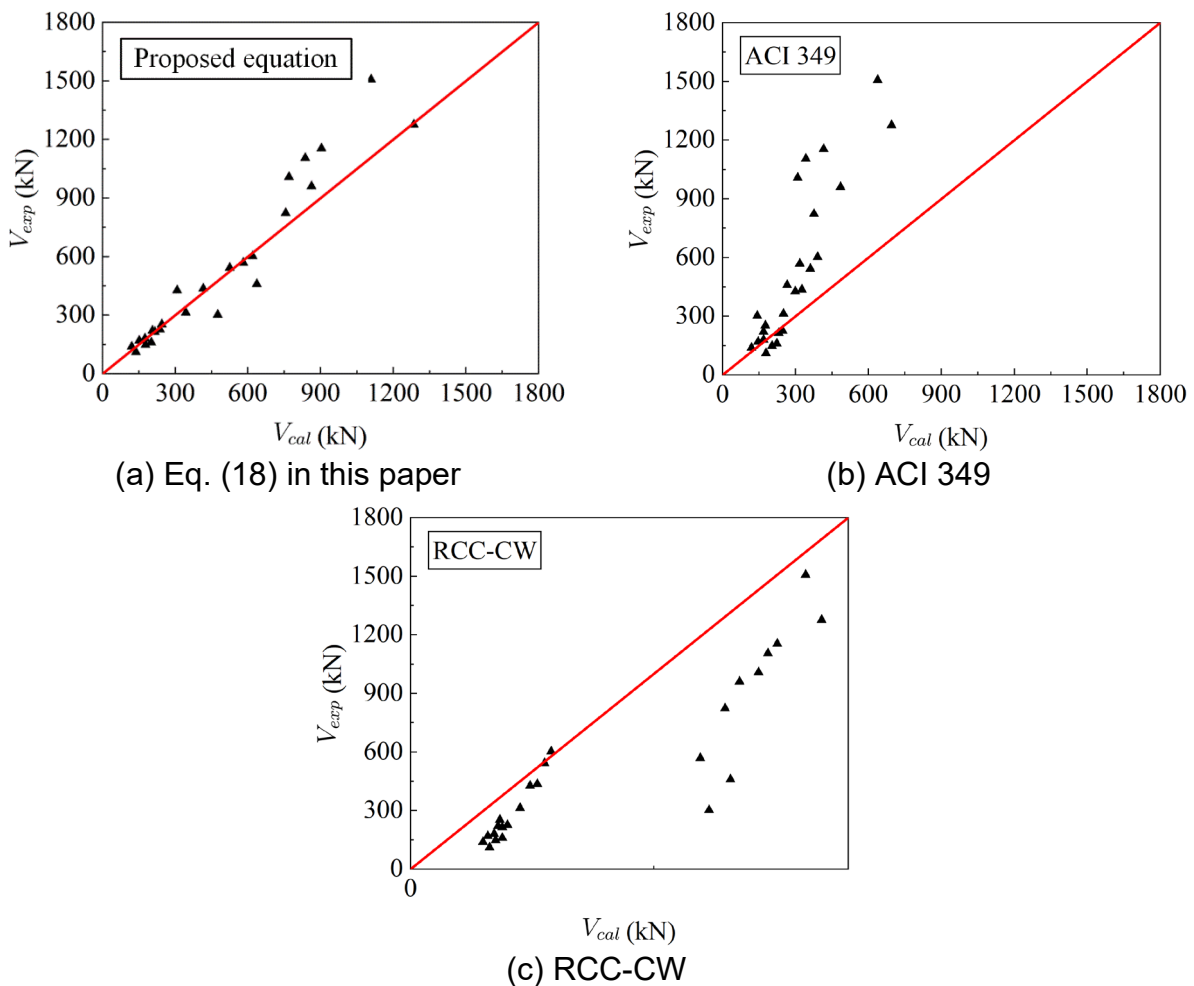


Fig. 6 Distribution of the ratio of calculated results to experimental results for the wall under vertical tension.

## 5 Conclusion

Based on the plastic limit theory, a calculation method for the in-plane lateral carrying capacity of low-rise reinforced concrete walls used in nuclear safety-related structures is established, and it is simplified and calibrated using experimental data to derive a simplified design equation. The following conclusions can be drawn:

(1) Under lateral and vertical loading, the low-rise reinforced concrete is subjected to positive stresses generated by vertical loads and bending and shear stresses generated by lateral loads.

(2) For the low-rise reinforced concrete wall, a combined mechanical model consisting of a diagonal shear surface and a shear friction surface can be established. The shear stress on the diagonal shear surface can be determined using the upper limit solution based on the plastic limit theory, and the shear stress on the shear friction surface can be calculated according to the shear friction theory.

(3) The proposed calculation equation for the in-plane carrying capacity of low-rise reinforced concrete walls is semi-theoretical and semi-empirical, and calculation results obtained by the proposed equation show good agreement with the test results. Moreover, its computational accuracy is better than that of the equation suggested in the codes ACI 349 and RCC-CW 2015.

## REFERENCES

- ACI 318-08 (2018), "Building Code Requirement for Structural Concrete", *ACI 318-08*, Farmington Hills, MI., ACI Committee.
- ACI 349-13 (2013), "Code Requirements for Nuclear Safety-Related Concrete Structures and Commentary", *ACI 349-13*, Farmington Hills, MI., ACI Committee.
- ASCE/SEI 43-05 (2005), "Seismic Design Criteria for Structures, Systems, and Components in Nuclear Facilities", *ASCE/SEI 43-05*, ASCE, American Society of Civil Engineers.
- Baek, J. W., Kim, S. H., Park, H. G. and Lee, B. S. (2020), "Shear-Friction Strength of Low-Rise Walls with 600 MPa Reinforcing Bars", *ACI STRUCT J*, **117**(1), 169-182.
- Gong, J. X., Sun, Y. L. and Zhang, N. L. (2018), "Study on in-plane shear of RC walls in nuclear power plant based on the plastic limit theory", *Building Structure*, **48**(16), 44-50.
- Gong, J. X., Sun, Y. L., Zhang, N. L. and Guo, S. H. (2022), Experimental and theoretical study of the constitutive relationship of the damaged reinforced concrete subjected to large aircraft crash. Dalian, Liaoning, Dalian University of Technology.
- Gulec, C. K. and Whittaker, A. S. (2011), "Empirical Equations for Peak Shear Strength of Low Aspect Ratio Reinforced Concrete Walls", *ACI STRUCT J*, **108**(1), 80-89.
- Gulec, C. K., Whittaker, A. S. and Stojadinovic, B. (2008), "Shear Strength of Squat Rectangular Reinforced Concrete Walls", *ACI STRUCT J*, **105**(4), 488-497.
- Hsu, T. T. C. and Mo, Y. L. (1985), "Softening of concrete in low-rise shearwalls", *Journal of the American Concrete Institute*, **82**(6), 883-889.
- Hwang, S. J. and Lee, H. J. (2002), "Strength prediction for discontinuity regions by softened strut-and-tie model", *J STRUCT ENG*, **128**(12), 1519-1526.
- Ji, X., Cheng, X. and Xu, M. (2018), "Coupled axial tension-shear behavior of reinforced concrete walls", *ENG STRUCT*, **167**(132-142).

*The 2023 World Congress on  
Advances in Structural Engineering and Mechanics (ASEM23)  
GECE, Seoul, Korea, August 16-18, 2023*

- Kassem, W. (2015), "Shear strength of squat walls: A strut-and-tie model and closed-form design formula", *ENG STRUCT*, **84**(430-438).
- Lefas, I. D. and Kotsovos, M. D. (1990), "Strength and deformation characteristics of reinforced-concrete walls under load reversals", *ACI STRUCT J*, **87**(6), 716-726.
- NB/T 20488-2018 (2018), "Performance based seismic design method for structures in nuclear facilities", *NB/T 20488-2018*, Beijing, China, National Energy Administration of China.
- Nie, X., Wang, J.-J., Tao, M.-X., Fan, J.-S., Mo, Y. L. and Zhang, Z.-Y. (2020), "Experimental Study of Shear-Critical Reinforced-Concrete Shear Walls under Tension-Bending Shear-Combined Cyclic Load", *J STRUCT ENG*, **146**(5).
- RCC-CW (2015), "Rules for design and construction of PWR nuclear civil works", *RCC-CW*, Paris, France, French Association for Design, Construction and In-Service Inspection Rules for Nuclear Island Components.